

# Adaptive View Planning for Aerial 3D Reconstruction of Complex Scenes

Cheng Peng, Volkan Isler

University of Minnesota, Twin Cities

**Abstract.** With the proliferation of small aerial vehicles, acquiring close up aerial imagery for high quality reconstruction of complex scenes is gaining importance. We present an adaptive view planning method to collect such images in an automated fashion. We start by sampling a small set of views to build a coarse proxy to the scene. We then present (i) a method that builds a view manifold for view selection, and (ii) an algorithm to select a sparse set of views. The vehicle then visits these viewpoints to cover the scene, and the procedure is repeated until reconstruction quality converges or a desired level of quality is achieved. The view manifold provides an effective efficiency/quality compromise between using the entire 6 degree of freedom pose space and using a single view hemisphere to select the views.

Our results show that, in contrast to existing “explore and exploit” methods which collect only two sets of views, reconstruction quality can be drastically improved by adding a third set. They also indicate that three rounds of data collection is sufficient even for very complex scenes. We compare our algorithm to existing methods in three challenging scenes. We require each algorithm to select the same number of views. Our algorithm generates views which produce the least reconstruction error.

## 1 Introduction

3D scene reconstruction has been an active research topic for more than two decades. The ability to obtain a rich and accurate 3D model of a scene is imperative for many applications including scene visualization, robot navigation, precision agriculture and image based rendering. Recently, with the prevalence of small and nimble aerial vehicles (drones), scene reconstruction from close-up aerial imagery has been gaining popularity. However, the battery and processing power of the drones also limit image acquisition for large scale, high quality reconstruction of complex scenes.

The most common method to obtain aerial imagery in an automated fashion is to use an off-the-shelf flight planner, such as Pix4D [1]. These planners generate simple zig-zag or circular trajectories for coverage. As we will show, these can be insufficient to produce high-quality 3D reconstructions especially in the case of low altitude flights over complex scenes. On the other end of the spectrum, there are *next-best-view* approaches, reviewed in the next section, which choose views actively so as to increase the amount of acquired information [2, 3].

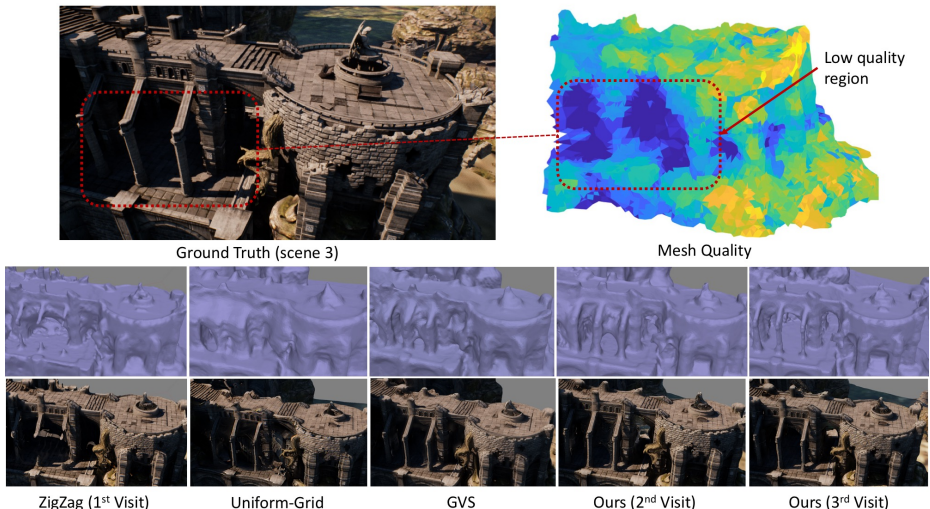


**Fig. 1.** The effect of view plans on reconstruction quality. The top left figure shows the scene. Bottom images provide a qualitative comparison of zigzag motion, uniform-grid method, greedy view selection, and our method after 2<sup>nd</sup> and 3<sup>rd</sup> visits. Rendered mesh and texture map views are shown to provide both structural and visual comparisons. Our method visually outperforms all other methods. The 3<sup>rd</sup> visit improves the reconstruction of low quality regions (top right) significantly.

These approaches are hard to implement on existing systems due to the need for significant onboard processing needed to accurately localize on the go with a real time SLAM approach [4–6], a decision making mechanism running on board to decide on the next best view and a controller to execute the strategy.

As a result, there has been recent interest in *explore-then-exploit* methods [7–9] for multi-stage image acquisition. These methods first “explore” the environment using a fixed trajectory (e.g. a zig-zag motion). The images are then used to build a rough mesh or voxel representation which is then used to plan an “exploit” trajectory that maximizes the coverage and accuracy of the scene in a second pass. Both trajectories are executed in an open loop fashion in the sense that no feedback from the images obtained during the flight is used. The advantage of this approach is that the secondary exploit visit to the scene has prior knowledge of the general geometry, making it possible to optimize for coverage and accuracy globally. Yet, it is easy to execute because the view points are generated offline and visited using a standard waypoint navigation algorithm.

In this paper, we propose a novel trajectory planning algorithm which takes this approach further. Our method iteratively refines the reconstruction quality while guaranteeing coverage. At the heart of our method is the reconstruction of a “view-surface manifold” for efficient view selection. The manifold adapts to the scene geometry which makes selection much more efficient than using a generic view grid or sphere. We present a method to construct an adaptive view manifold

that significantly reduces the search space. We also present an iterative approach to plan views by systematically revisiting low quality regions. Our results provide two key insights illustrated qualitatively in Figure 1: (1) For complex scenes, a standard zig-zag trajectory may fail to provide good enough views even for an initial scene estimate. (2) We show in experiments that 3 visits are often sufficient and sometimes necessary to obtain high quality reconstructions.

## 2 Related Work

The view selection problem remains an essential topic for 3D reconstruction. One of the early view selection methods optimizes the baselines among a set of images for accurate depth reconstruction [10]. Maver and Bajcsy [11] utilized the knowledge of contours and occlusions to choose views. Scott et al. [12] later analyzed the view selection problem for reconstruction in detail and showed that it is an NP-Complete problem. This line of work is called active vision because the views are managed actively to improve reconstruction quality [13]. Scott et al. [12] utilize an integer programming method to solve for the view planning problem. Vasquez et. al. [2] propose a greedy selection method that optimizes for the next-best-view for reconstruction.

To obtain a high quality 3D reconstruction, many methods have been proposed to address view selection problem. Snavely et al. [14] propose a method called “skeleton set” to reduce the input images by selecting a subset of frames from the image graph. Similarly, image clustering methods [15–19] are proposed to find an iconic image for representation. Kaucic et al. [20] assume planar scene models and speed up the optimization using factorization [21]. Peng and Isler [22] analyze the reconstruction quality by modeling the uncertainty as a cone and propose a coarse-to-fine strategy to reduce the number of views.

To reduce the view search space, the view sphere method [23] is proposed to limit the view selection around an “enclosing” sphere to the object. However, a single view sphere cannot handle large scaled scenes. Therefore, some methods [7, 8] discretize the 3D viewing space for aerial 3D reconstruction. Instead of choosing the views in 3D space, we propose an adaptive 2D view manifold that reduces the search space from 3D to 2D.

Since the scene is initially unknown, an initial geometry estimation [7, 8, 15] is performed for view planning in the next phase. Our method improves upon this approach by identifying regions with low reconstruction quality and iteratively visiting the scene for refinement.

## 3 Technical Overview

In order to reconstruct a scene, we need to plan an optimal trajectory that covers the scene with high quality.

We decompose the trajectory planning problem into two subproblems. First, we find a sparse set of views that ensures coverage. Second, a trajectory that visits these views are constructed.

Our method adopts the idea of *explore-then-exploit* and improves upon it by limiting the view search space to a smooth manifold with multiple visits for refinement. Initially, a zig-zag flight motion is deployed to cover the scene. We build a sparse point cloud with surface mesh [24] that generalizes the scene geometry. Based on the surface mesh, we identify the low quality regions for refinement in the next trajectory planning iteration.

Given the estimated scene geometry, we then plan a small set of views to ensure coverage by relaxing the visibility constraints. We call those initial views *skeleton views*. The skeleton views are extracted from a viewing surface that adapts to the scene geometry called *the view manifold*, which reduces the view search space from 3D to a 2D manifold.

The next step is to find an efficient path that visits the skeleton views while ensuring reconstruction quality. We formulate this problem as a Traveling-Salesman-Problem with weighted distance. The weight between two skeleton views represents the quality gain of each view along that path. Therefore, it forces the trajectory to cover regions with low quality.

For many regions that cannot be well-represented by the initial mesh, more than 2 visits to the scene are necessary, where the second trajectory can provide better scene proxy for view selection. Since we only identify regions of low quality for refinement, the repeated visits only increase the total views by a small fraction.

## 4 Notations and Definition

In this section, we formalize the view selection problem and present our notation. Given a triangular mesh  $\mathcal{M} = \{\mathcal{F}, \mathcal{V}\}$  built on a point clouds  $\mathcal{G} = \{g_1, g_2, \dots, g_G\}$  with mesh vertices  $\mathcal{V} = \{v_1, v_2, \dots, v_V\}$  and a set of faces  $\mathcal{F} = \{f_1, f_2, \dots, f_F\}$ ,  $f_i \in \mathcal{V} \times \mathcal{V} \times \mathcal{V}$ , we would like to plan a trajectory with a minimum set of views  $C = \{c_1, c_2, \dots, c_C\}$ ,  $c_i \in \mathbb{R}^6$  that covers  $\mathcal{F}$  with good quality, where the quality measure is defined in Section 4.2. Here, a camera view  $c$  consists of 6 degree-of-freedom with  $P_c \in \mathbb{R}^3$  for position and  $R_c \in \mathbb{R}^3$  for rotation. For each face of the mesh  $f \in \mathcal{M}$ , we define  $N_f$  and  $N_v$  as the normal vector of the face  $f$  and vertex  $v$  respectively. We also define the center of the face as  $P_f$ .

### 4.1 Visibility Cone Model

In order to define the coverage of a scene, we first need to model the visibility of a face so that we can reason for the coverage of the scene.

We model the visibility of each face of the mesh as a right circular cone denoted as  $Cone(f)$  shown in Fig 2. If a view  $c$  is within the visibility cone  $Cone(f)$ , the face  $f$  is visible from the view  $c$ . Because the scene is not fully known, we build the cone based on the existing views and infer the visible region with this model. Therefore, the cone apex angle denoted as  $\Theta(f)$  is

$$\Theta(f) = \max_{c_i, c_j \in C_{init}} \angle(\overline{P_f c_i}, \overline{P_f c_j}) \cdot I(f) \quad (1)$$

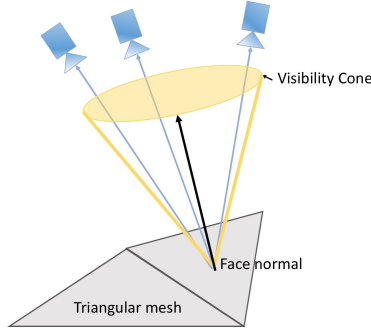


**Fig. 2.** Visibility cone of a triangular mesh: the visibility cone infers the region of possible good views for the triangular mesh.

where  $I(f)$  is an indicator function.  $I(f) = 1$  if and only if  $c_i, c_j$  construct the face  $f$ .  $C_{init}$  is the initial set of views that construct the scene.  $\Theta(f)$  is defined as the *visibility angle* of the face  $f$ . The cone axis is set to the face normal  $N_f$ .

The coverage of the scene is defined such that for each face  $f \in \mathcal{F}$ , there are at least two views  $\{c_i, c_j\} \in Cone(f)$  within the visibility cone. The reconstruction quality is then defined as the angle between the camera pair  $\{c_i, c_j\}$  with the face center  $P_f$ . In practice, high reconstruction quality requires not only the angular constraint but also the number of visible cameras. In Section 4.2, we incorporate these criteria to measure region quality.

However, the initial estimated mesh may contain bad faces that do not represent the true surface. Therefore, we provide an adaptive method that improves those faces iteratively.

## 4.2 Reconstruction Quality

Low reconstruction quality regions are generally the regions that do not contain accurate points to be triangulated. Visually, the mesh or texture representation captures a much distorted geometry compared to reality. Those low quality regions are either occluded or low texture regions that cannot receive sufficient good views. For a complex scene, occluded and low-texture regions are hard to reconstruct without region-specific view planning. Therefore, we identify those regions in our model and plan the views only for the low quality region for refinement. It is much more efficient than planning the views for the entire scene.

The reconstruction quality is mainly effected by two factors: the parallax between the camera pair and the number of views that reconstruct the region. Generally speaking, high parallax results in accurate triangulation while being hard to find feature correspondences. More views can increase the number of correctly matched features per region. Therefore, we define the quality  $Q(f)$  of

each face  $f$  in the mesh as follows.

$$Q(f) = \Theta(f) \cdot \frac{|\kappa(f)|}{Area(f)} \quad (2)$$

where  $\kappa(f) = \{c | c \in Cone(f)\}$  is a set of views that are inside visibility cone of  $f$ . Essentially, the quality measure  $Q(f)$  is the average number of visible cameras per face area weighted by the visibility angle.

## 5 View Planning Method

In this section, we introduce our approach in detail. The coverage and quality of the reconstruction both require at least 2 views with common cover region and enough parallax. This problem can be viewed as a set cover problem that finds the minimum number of views such that their common region covers the entire scene, which is shown to be NP-Complete [25]. The problem is further complicated by optimization over both position and orientation for each view. In real applications, more than 2 views are desired to eliminate the matching error per region, which adds another layer of difficulty.

To approach the view planning problem, we decouple it into two sub-problems of finding the positions and the orientations separately from an adaptive search space.

### 5.1 View Manifold

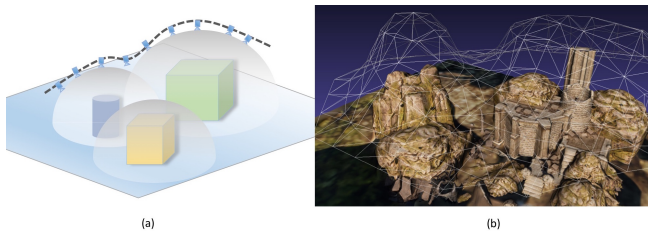


**Fig. 3.** The view manifold: (a) View spheres for multiple objects can be combined into the view manifold. (b) The texture map of scene 2 with the adaptive “enclosing” manifold shown as the white mesh.

We propose a novel method that reduces the view search space from 3D to a 2D manifold. Instead of discretizing  $P \in \mathbb{R}^3$  into grids [7], we choose a set of views on a surface that adapts to the scene.

In conventional methods [23], a viewing sphere is imposed around an object for view planning. However, such a viewing sphere treats the surface of the objects from different distances, which may fail to reconstruct multiple objects due to limitations of image resolution.

We generalize the viewing sphere method and improve upon it to adapt to more complex scenes using the viewing manifold. From the work of Peng and Isler [22], they prove that for a planar region, one can use a small number of cameras lying on a viewing plane parallel to the ground plane to guarantee coverage and quality. Similarly, in a more complex scene, we can extract such an adapting view manifold.

**Manifold Construction** We can impose a viewing half hemisphere for each face of the mesh. For the entire scene, the adapting view manifold is constructed as the outer surface of the union of those half hemispheres. Notice that it obtains a similar geometry as the scene mesh itself. However, the manifold must somehow “enclose” the scene with certain distance while avoiding intersection with the scene. Therefore, we build the view manifold based on the existing scene mesh  $\mathcal{M}$ .

Given a mesh  $\mathcal{M}$  of the scene with vertices  $\mathcal{V}$ , we expand each vertex for a predefined distance  $d$  in the direction of their normals and generate a new set of vertices  $\mathcal{V}' = \{v' | v' = v + dN(v)\}$ . We identify the exterior set of vertices  $E(\mathcal{V}')$  and build a smooth surface denoted as  $\partial(E(\mathcal{V}'))$  as shown in Fig 3(a). We call this surface *the view manifold*. For a single convex object, the resulting view manifold will resemble a viewing sphere. However, for more complex scenes, our view manifold can adapt to convex and concave regions.

The given mesh of the scene  $\mathcal{M}$  needs to be smoothed so that the surface normals are consistent. The initial estimated mesh does not depict the scene well. Thus some regions can have arbitrary bad triangular mesh that leads to inconsistent distribution of vertices for the view manifold. Such inconsistency also motivates us to visit the scene iteratively for refinement. In section 5.2, we also smooth the scene mesh to produce consistent visibility cone axes for the same reason.

## 5.2 The Selection of Skeleton Views

There are many different ways to find a set of views from the search space. In case for the viewing sphere, a uniform sampling method is used for the best view candidates. There are other methods [2, 8, 9, 12, 25] that optimize some cost function to search for the best set of views. Since we can infer the visible views using the visibility cone, the coverage and quality objective can be translated into finding the minimum number of views such that there are at least  $k$  views with minimum spacing in each of the visibility cone of the mesh.

A coarse-to-fine view selection method [22] is proposed to cover all the faces with good quality. The idea is to reduce the number of views by selecting a set of view grids with increasing resolution so that fewer views are required for simple regions. However, given the small visibility angle of each face, the resulting views can be too dense to plan a trajectory.

We improve upon this idea by coarsening the visibility angle of each face, which results in a sparse set of views called *the skeleton views*. During the trajectory planning (Section 5.4) phase, the actual visibility angle for each face

will be incorporated to encourage motion through low quality region for better coverage.

### 5.3 View Orientation

Once the skeleton views are selected, we now need to find the orientation for each view point. In order to maximize the reconstruction quality, we optimize the view orientation to cover the low quality regions as follows.

$$R_c = -\frac{1}{|\chi(c)|} \sum_{f \in \chi(c)} \frac{N_f}{Q(f)} \quad (3)$$

where  $\chi(c) = \{f | c \in \text{Cone}(f)\}$  is a set of faces  $f$  such that  $c \in \text{Cone}(f)$ . We also weight the face normal by the region quality measure  $Q(f)$  so that we orientate more towards the low quality region.

### 5.4 Trajectory Planning

Given the skeleton views on the manifold, we plan our trajectory through those views with the shortest path. However, we want the trajectory to also go through regions with low quality to ensure better coverage. Therefore, we propose a weighted distance function that penalizes motions through high quality regions. For each view  $c$  with orientation  $R_c$ , we define the gain of the view as the total region quality.

$$\text{Gain}(c) = \sum_{f \in \chi(c)} Q(f) \quad (4)$$

The distance weight between two skeleton views  $\{c_i, c_j\}$  are then defined as such:

$$w(c_i, c_j) = \sum_{c \in S_{ij}} \text{Gain}(c) \quad (5)$$

where  $S_{ij}$  is a set of intermediate views along the straight line path between  $\{c_i, c_j\}$ .

## 6 Results

In order to evaluate our method, we use a high-quality visual rendering software, Unreal Engine [26]. It is a game development engine that produces photo-realistic scenes. We conduct our experiment in the synthetic environment by controlling a virtual camera using the UnrealCV Python Library [27]. We tested our method of view planning in 3 different synthetic scenes (from GRASS LAND [28] and OIL Refinery [29] datasets) that contain occluded regions from the top view. We compare our reconstruction results both qualitatively and quantitatively among that of three baseline methods. Qualitatively, we show both the mesh and the texture map to demonstrate the visual completeness of the reconstruction. Quantitatively, we perform both accuracy and coverage test using the dense reconstruction results with the ground truth depth data.



## 6.1 Implementation Details

We perform dense reconstruction, mesh generation and texture mapping using a commercial software Agisoft [30]. For each scene, the initial zigzag coverage spacing is set to 1 meters and 20-30 meters above the scene. The total number of input images are 100-250 images depending on the size of the scene. The dense reconstruction is set to medium-quality in Agisoft.

**View Manifold** To generate the view manifold, we use the MeshLab software [31] with the Screened Poisson Reconstruction Algorithm [24]. We select the octree depth to be 5 for a coarser mesh and select a uniform sampling of points using Poisson-disk Sampling option with a total of 20000 points. Then, we expand those sampled points for a fixed distance  $d$  in the direction of their normals. The distance is set to a fix value such that the top of the manifold touches the initial viewing plane. To filter out points within the manifold, we define a visibility cone for each point with apex angle set to  $30^\circ$  with normal direction the opposite as their normals. Therefore, any points within such cone will be deleted. We then built a surface from those points as shown in Fig 3 (b) (Screen Poisson Reconstruction method with octree depth of 8) and sample 20000 points (Poisson-disk Sampling) on the surface as potential view candidates on the manifold.

**Skeleton Views** Before selecting the skeleton views, we first smooth the face normals for the mesh based on the neighbor face normals. Then the visibility angle  $\Theta(f)$  of face  $f$  is set to  $30^\circ$ , which produces 20-50 skeleton views on the manifold depending on the scenes.

**Trajectory Planning** To estimate the shortest path traveling among the skeleton views, we use the Concorde-TSP solve [32]. In Eq 5, we picked the intermediate views every 0.1 meters, where their view orientations are interpolated. We only estimate the weight for the nearest 5 views to avoid traveling too far for coverage.

## 6.2 Comparison Methods

To compare our view planning algorithm, we build three different baseline methods. There is no benchmark dataset that allows active view selection for large scale aerial 3D reconstruction. Therefore, we generalize the core idea from other methods and implemented our representative versions.

**ZigZag** The basic trajectory to cover a scene is a zigzag motion. We plan this motion with a predetermined height that fully covers the scene. The zigzag motion is available using a commercial flight planner such as Pix4D [1].

**Uniform-Grid** Aside from the basic zigzag motion, another naive baseline method is to reconstruct a uniformly spaced sparse views in 3D viewing space. We construct this Uniform-Grid method in a discretized 3D viewing space. The number of those sparse views will be set to be equal to that of the skeleton views for comparison. To compare with our view manifold approach, we optimize the view orientations and trajectory from those sparse view set using our method.

**Greedy View Selection** Many different methods [7, 8] model the cost function in view planning problem as a submodular function, where the views are selected using the greedy algorithm. Therefore, we implement a naive Greedy View Selection(GVS) method to compare with our method. We model the gain of a view using our previous Eq 4. Given a set of views  $S \subseteq C$ , the marginal gain of an additional view  $c$  is the following.

$$Gain(c, S) = \sum_{f \in \chi(S \cup c) - \chi(c)} Q(f) \quad (6)$$

where  $S \subseteq C$  is subset of views in  $C$  and  $\chi(S)$  is the faces covered by the view set  $S$ .

The GVS method has access to the view manifold and selects the next best view using Eq 6 from its neighbor views. We define the neighbor views to be within 1 meter. The GVS method starts from a random view point and terminates when the total number of views exceeds that of our algorithm.

### 6.3 Qualitative Comparison

As shown in Fig 1 and Fig 6, we can see that our method out performs all other methods. In Fig 1, the third visits to the same scene shows significant improvements of the low quality regions. Those improved regions are not reconstructed from the initial scene, which is only identified through the second visit to the scene. It validates our assumption that the initial estimated geometry is too coarse for view planning. A closeup comparison is shown in Fig 6. It is evident that our method produced significantly better structure.

We also show that the number of views for each iterative visit as shown in Fig 4. The first iteration is the standard zigzag motion. We can see that the 3<sup>rd</sup> and 4<sup>th</sup> visits only add less than 40 views to the 2<sup>nd</sup> visit. The small increment in the number of views means the low quality regions are well covered after the 2<sup>nd</sup> and 3<sup>rd</sup> iteration. If the low quality regions appear far apart, the trajectory will contain only views for the desired regions. Therefore, the input number of views is only dependent on the area of the low quality region.

### 6.4 Quantitative Comparison

We compare the reconstruction results quantitatively using the absolute depth error since the true depth can be obtained from UnrealCV Python Library [27]

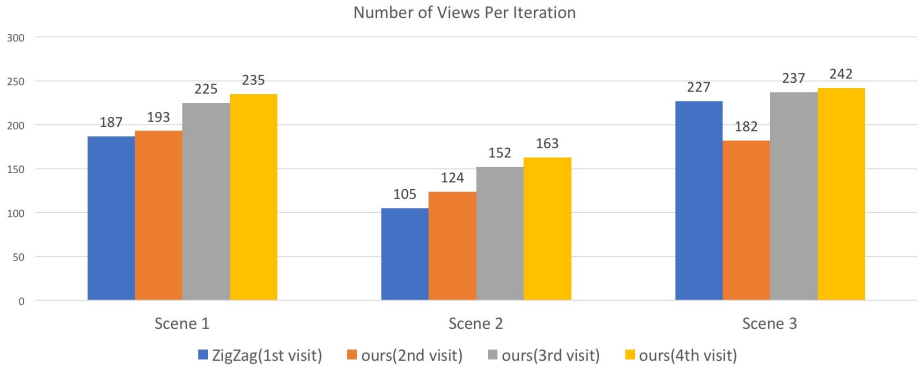


**Fig. 4.** The number of input images at each iteration: the first iteration is the standard zigzag motion. We can see that the  $3^{rd}$  and  $4^{th}$  visits only add less than 40 views to the  $2^{nd}$  visit. The small increment in the number of views means that the low quality regions are well covered after the  $2^{nd}$  and  $3^{rd}$  iteration

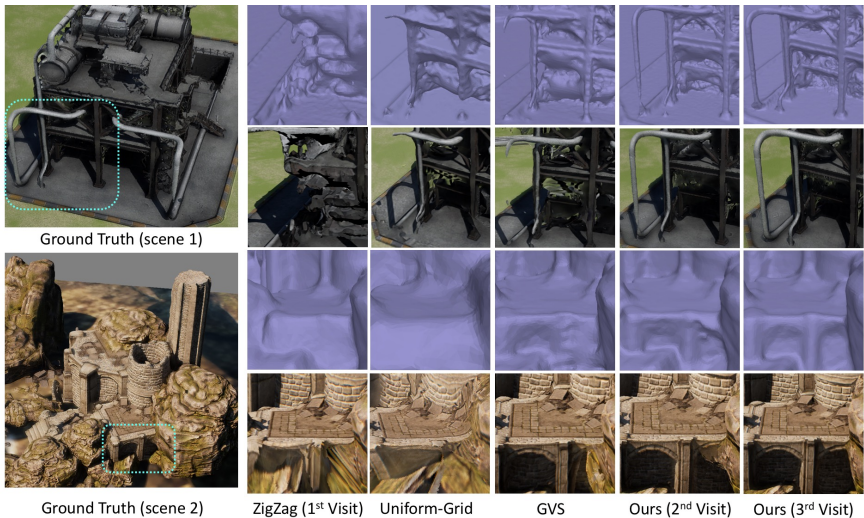


**Fig. 5.** Qualitative comparison of the reconstruction among zigzag motion, uniform-grid method, greedy view selection, and our method for the  $2^{nd}$  and  $3^{rd}$  visits. Both the rendered mesh and texture map are shown to provide both structural and visual comparison. Our method out performs all other methods, where the  $3^{rd}$  visit improves the structure further more.

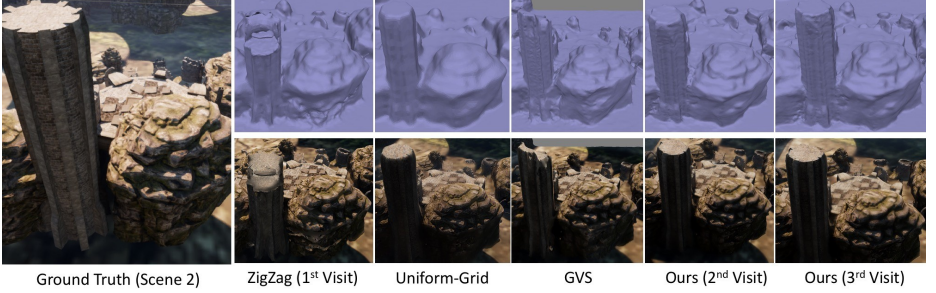


**Fig. 6.** Qualitative comparison of the reconstruction among zigzag motion, uniform-grid method, greedy view selection, and our method for the  $2^{nd}$  and  $3^{rd}$  visits. Both the rendered mesh and texture map are shown to provide both structural and visual comparison. Our method out performs all other methods, where the  $3^{rd}$  visit improves the structure further more.

**Table 1.** The comparison of depth error and completeness

Methods	Depth Error Avg(mm)	Depth Error Std(mm)	Completeness(%)
ZigZag	211.5	203.4	14.5%
Uniform-Grid	189.3	143.5	19.3%
GVS	143.9	120.3	18.4%
<b>ours(<math>2^{nd}</math> visit)</b>	<b>123.2</b>	<b>105.6</b>	<b>28.6%</b>
<b>ours(<math>3^{rd}</math> visits)</b>	<b>109.5</b>	<b>102.1</b>	<b>29.1%</b>

in the simulation environment. The quantitative comparison of the reconstruction are shown in Table 1. We estimate the accuracy and coverage of the scene using the depth accuracy and dense point clouds completeness defined here. For accuracy, we calculate mean and standard deviation of the depth on the corresponding pixel from estimated dense point clouds and the ground truth depth image. The completeness is defined as the ratio between the number of pixels that contains the depth from dense point clouds and that of the ground truth. To analyze the depth from our scene, we filter out pixels that are more than 50 meters away in the ground truth. Since we are selecting only the medium-quality for our dense point clouds, the resulting completeness percentage can only be as high as 35%.

As shown in Table 1, the our method achieves the lowest depth error with the highest completeness percentage. Note that the  $3^{rd}$  visit only increase the completeness of the  $2^{nd}$  visit by less than 1%. This is because most of the scene is already covered and the additional iteration only increase the corresponding accuracy of the scene.

## 7 Conclusion

This paper studies the problem of view selection for aerial 3D reconstruction. We propose an adaptive view planning method to reconstruct a complex scene

from aerial imagery. Our work has two novel aspects: First, we present a method to reduce the view search space to a 2D view manifold. This view manifold generalizes the idea of using view sphere for a single object to more complex scenes. Second, we identify low reconstruction quality regions to plan our next set of views iteratively. We observe that the initial scene proxy reconstructed from the standard zigzag motion can be insufficient for planning. Therefore, more than 2 iterations of view planning are sometimes necessary to build a high quality reconstruction. At the same time, we show that three sets of views are sufficient to produce a high quality reconstruction.

We compared our view planning method with 3 baseline methods using ground truth obtained from a photo-realistic rendering software (Unreal Engine). The first baseline algorithm is the basic zigzag motion on a plane. The second method (Uniform-Grid) chooses the views from the 3D viewing space instead of the our view manifold. The last method choose the views greedily to maximize the information gain. Our method outperforms the baseline methods both qualitatively and quantitatively.

## References

1. Pix4D: Pix4Dcapture. <https://pix4d.com/product/pix4dcapture/>
2. Vásquez, J.I., Sucar, L.E.: Next-best-view planning for 3d object reconstruction under positioning error. In Batyrshin, I., Sidorov, G., eds.: *Advances in Artificial Intelligence*, Berlin, Heidelberg, Springer Berlin Heidelberg (2011) 429–442
3. Dunn, E., Frahm, J.M.: Next best view planning for active model improvement. In: 2009 20th British Machine Vision Conference, BMVC 2009, British Machine Vision Association, BMVA (2009)
4. Mur-Artal, R., Montiel, J.M.M., Tardos, J.D.: Orb-slam: a versatile and accurate monocular slam system. *IEEE Transactions on Robotics* **31**(5) (2015) 1147–1163
5. Klein, G., Murray, D.: Parallel tracking and mapping for small ar workspaces. In: *Mixed and Augmented Reality, 2007. ISMAR 2007. 6th IEEE and ACM International Symposium on*, IEEE (2007) 225–234
6. Engel, J., Schöps, T., Cremers, D.: Lsd-slam: Large-scale direct monocular slam. In: *European Conference on Computer Vision*, Springer (2014) 834–849
7. Roberts, M., Dey, D., Truong, A., Sinha, S.: Submodular trajectory optimization for aerial 3d scanning. In: *International Conference on Computer Vision*
8. Hepp, B., Nießner, M., Hilliges, O.: Plan3d: Viewpoint and trajectory optimization for aerial multi-view stereo reconstruction. *arXiv preprint arXiv:1705.09314* (2017)
9. Hoppe, C., Wendel, A., Zollmann, S., Pirker, K., Irschara, A., Bischof, H., Kluckner, S.: Photogrammetric camera network design for micro aerial vehicles
10. Farid, H., Lee, S.W., Bajcsy, R.: View selection strategies for multi-view, wide-baseline stereo. (1994)
11. Maver, J., Bajcsy, R.: Occlusions as a guide for planning the next view. *IEEE transactions on pattern analysis and machine intelligence* **15**(5) (1993) 417–433
12. Scott, W.R., Roth, G., Rivest, J.F.: View planning for automated three-dimensional object reconstruction and inspection. *ACM Computing Surveys (CSUR)* **35**(1) (2003) 64–96
13. Chen, S., Li, Y., Wang, W., Zhang, J.: Active sensor planning for multiview vision tasks. (2008)

14. Snavely, N., Seitz, S.M., Szeliski, R.: Skeletal graphs for efficient structure from motion. In: Computer Vision and Pattern Recognition, 2008. CVPR 2008. IEEE Conference on, IEEE (2008) 1–8
15. Hornung, A., Zeng, B., Kobbelt, L.: Image selection for improved multi-view stereo. In: Computer Vision and Pattern Recognition, 2008. CVPR 2008. IEEE Conference on, IEEE (2008) 1–8
16. Mauro, M., Riemenschneider, H., Signoroni, A., Leonardi, R., Van Gool, L.: An integer linear programming model for view selection on overlapping camera clusters. In: 3D Vision (3DV), 2014 2nd International Conference on. Volume 1., IEEE (2014) 464–471
17. Li, X., Wu, C., Zach, C., Lazebnik, S., Frahm, J.M.: Modeling and recognition of landmark image collections using iconic scene graphs. In: European Conference on Computer Vision, Springer (2008) 427–440
18. Mauro, M., Riemenschneider, H., Van Gool, L., Leonardi, R.: Overlapping camera clustering through dominant sets for scalable 3d reconstruction. In: Proceedings BMVC 2013. (2013) 1–11
19. Ladikos, A., Ilic, S., Navab, N.: Spectral camera clustering. In: Computer Vision Workshops (ICCV Workshops), 2009 IEEE 12th International Conference on, IEEE (2009) 2080–2086
20. Kaucic, R., Hartley, R., Dano, N.: Plane-based projective reconstruction. In: Computer Vision, 2001. ICCV 2001. Proceedings. Eighth IEEE International Conference on. Volume 1., IEEE (2001) 420–427
21. Sturm, P., Triggs, B.: A factorization based algorithm for multi-image projective structure and motion. In: European conference on computer vision, Springer (1996) 709–720
22. Peng, C., Isler, V.: Optimal reconstruction with a small number of views. CoRR **abs/1704.00085** (2017)
23. Vásquez-Gómez, J.I., López-Damian, E., Sucar, L.E.: View planning for 3d object reconstruction. In: Intelligent Robots and Systems, 2009. IROS 2009. IEEE/RSJ International Conference on, IEEE (2009) 4015–4020
24. Kazhdan, M., Hoppe, H.: Screened poisson surface reconstruction. ACM Transactions on Graphics (ToG) **32**(3) (2013) 29
25. Tarbox, G.H., Gottschlich, S.N.: Planning for complete sensor coverage in inspection. Computer Vision and Image Understanding **61**(1) (1995) 84–111
26. UnrealEngine: Unreal Engine 4. <https://www.unrealengine.com/en-US/blog>
27. Qiu, W., Yuille, A.: Unrealcv: Connecting computer vision to unreal engine. In: European Conference on Computer Vision, Springer (2016) 909–916
28. Games, E.: Infinity Blade: Grass Land. <https://www.unrealengine.com/marketplace/infinity-blade-plain-lands> (2015)
29. Team, C.D.: Oil Refinery Pack. <https://www.unrealengine.com/marketplace/oil-refinery-pack> (2017)
30. Agisoft: Agisoft. <http://www.agisoft.com/>
31. Cignoni, P., Callieri, M., Corsini, M., Dellepiane, M., Ganovelli, F., Ranzuglia, G.: MeshLab: an Open-Source Mesh Processing Tool. In Scarano, V., Chiara, R.D., Erra, U., eds.: Eurographics Italian Chapter Conference, The Eurographics Association (2008)
32. Applegate, D., Bixby, R., Chvatal, V., Cook, W.: Concorde TSP solver. URL: <http://www.math.uwaterloo.ca/tsp/concorde.html> (2017)